EFECT OF A DEFECT IN THE DEHIDRAL ANGLE ON ELECTRONIC AND OPTICAL PROPERTIES OF TRIGONAL SELENIUM

Mekahlia MAHIRA[1], Benkhedir Mohammed LOUTFI[1], Belghit RAFIK[2]

Amorphous Selenium is gaining interest as it is used as X-ray sensitive layer in X-ray digital imaging machines and high-sensitivity HARPICON cameras used in low light intensity conditions. The density of states (DOS) in pure a-Se contains a shallow defect level at ~ 0.25 eV above the top of the valence band (Ev) and another shallow defect at 0.3 eV below the bottom of the conduction band (Ec). These levels are thought to be due to a defect in the dihedral angle in Se chains. In this paper we propose to study the electronic and optical properties of trigonal Se (t-Se) and t-Se containing a defect (t-Se(D)) in the dihedral angle using the WIEN2k code based on the density functional theory (DFT) using the General Gradient Approximation (GGA) with and without the potential of correction Tran and Blaha modified Becke-Jhonson (TB-mBJ). The density of states shows that the gap of t-Se containing the defect is about 0.2 eV less than the t-Se. the changes are mostly caused by the change in the p-orbital. The real and imaginary parts of the dielectric constant show changes that can be explained by the distribution of charge density around atoms that reflects the nature of bonds.

Keywords: Selenium, defects, ab initio

1. Introduction

Selenium (Se) is regaining interest because it has found new applications. In the digital x-ray imaging Se is used as a photosensitive layer in amorphous Selenium (a-Se) based flat-panel x-ray detectors [1, 2]. In high-sensitivity TV cameras a-Se is used as photosensitive layer in high-gain avalanche rushing amorphous photoconductor (HARP) films [3]. In the two previous applications the photosensitive layer, that is a-Se, is used under a high applied voltage. However crystalline Selenium (c-Se) is a good candidate as a photosensitive material for image sensors running under lower applied voltage [4]. This advantage gives more flexibility to use current CMOS technology in the readout circuit [4-5].

[1] Laboratoire de physique appliqué et théorique, Université de Tébessa, Tébessa, Algérie, e-mail: mekahlia.maha.2014@gmail.com, e-mail: mohamed.benkhedir@univ-tebessa.dz
[2] Laboratory Studies of Surface and Interfaces of Solid Materials (LESIMS), Department of Physics, Faculty of Sciences, University Badji Mokhtar, P.O. Box 12, Annaba 23000, Algeria, e-mail: rafikchr@gmail.com

Selenium can exist in different phases (monoclinic: α, β and γ, rhombohedric, orthorhombic, hexagonal, α- and β-cubic…) at the normal conditions of temperature and pressure, the most stable phase is the hexagonal one [6, 7]. As mentioned above, a-Se is the most used form of Se in the recent applications. In short range order a-Se has the same structure as the crystalline one, however; at long range order the periodicity is lost [8]. The amorphous form of a material is essentially the consequence of small changes in bond lengths and angles that are the topological defects [8]. The hexagonal phase of Se, or t-Se, is formed of parallel helical chains. A change in the sense of rotation of the helical chains at one atom introduces a change of the direction of dihedral angle, which is the angle between two adjacent planes formed of two successive bonds [9]. This defect puts the lone pairs of two successive atoms likely parallel rather than perpendicular [9] and this introduces a positive repulsive energy in the system. This neutral defect is believed to be the explanation for two shallow defect levels as deduced from the interpretation of different experimental results. The energetic levels of this defect are located, in the gap states of a-Se, at about 0.25 eV from the valence and conduction band edges [10-13]. However, some other studies based on other experimental results show that the DOS of a-Se above the valence band edge is featureless [14]. The charge carriers trapping in the gap states has a hard impact on the devices, as shown for example in the case of amorphous selenium direct conversion avalanche X-ray detectors [15]. Thus it is very important to know the real distribution of gap states in selenium. It will be fruitful to approach the problem using theoretical methods in order to elucidate the DOS structure of a-Se, especially the shallow defect levels.

The well known density functional theory (DFT) approach is widely used to calculate structural and electronic properties of semiconductors that are the starting point to calculate other physical properties such as the optical and mechanical ones. Recently, David Koller and coworkers have proposed the modified Becke Johnson exchange potential (TB-mBJ) to be used as a correction to the potential in order to calculate accurate electronic band structures for semiconductors and insulators. This approach has proved its validity, and it permits to get values of the gap close to the experimental ones at a low cost [15].

In this paper we propose to study the effect of a defect in the dihedral angle on the structural, electronic and optical properties of t-Se. For this purpose, we used the full potential linearized augmented plane wave (FP-LAPW) method with the TB-mBJ correction potential [16].

2. Theoretical methods

In this study we have used the full-potential linearized augmented plane-wave (FP-LAPW) as implemented in the WIEN2k code [17] based on the density

functional theory (DFT). We have, also, used the Perdew-Burke-Ernzerhof parameterization of the Generalized Gradient Approximation (GGA) [18] that has been chosen as an approximation of exchange-correlation potential [18]. The GGA approximation was used to study the structural properties; while the Tran and Blaha modified Becke Johnson (TB-mBJ) potential correction [16] was added to the GGA potential to study the electronic and optical properties of our systems. The separation between the core and valence electrons was set to -6 Ry. Where the cutoff parameter $R_{MT}K_{max}$ = 7 (R_{MT} is the smallest radius of the muffin-tin spheres and K_{max} is the magnitude of the largest wave vector in the first irreductible Brillouin zone). We have used 200 k-point to sample the Brillouin zone. The self-consistent calculations converge when the difference in the calculated total energy is less than 10^{-4} Ry.

3. Results and discussion

3.1. Structural properties

As mentioned above, the most stable phase of Selenium is the trigonal one. The t-Se has the group of symmetry P3121 and has 3 atoms in the primitive cell. The structural study of t-Se using GGA approximation and the Murnagan equation [19] showed that the cell parameters have the values a = 4.4261 Å and c = 5.0706 Å. The obtained results are in good agreement with other experimental and theoretical studies as shown in Table 1. We used the t-Se primitive cell to construct a 2x2x2 super cell containing 24 atoms thus we optimized the super cell structure in the same previous way and found that the cell parameters are a = 8.8375 Å and c = 10.171 Å. Moreover, we relaxed the structure to get the Se atom positions in the super cell. We constructed a super cell containing a dihedral defect by changing the sign of the dihedral angle at the atoms number 22 and 23 as shown in Fig. 1b.; Fig. 1a. shows a super cell without the dihedral defect.

The dihedral defect does not change the lattice parameters and the symmetry; however the positions of atoms change.

Table1

The calculated structural parameters of t-Se

	Lattice parameters (Å)		References
	a = b (Å)	c (Å)	
Our calculation	4.4261	5.0706	
GGA	4.544	5.055	[20]
LDA	3.879	5.080	[20]
Experimental	4.3662	4.9536	[21]

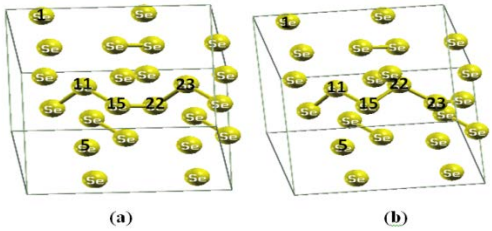

Fig. 1. The crystal structures of t-Se (a) and t-Se(D) (b).

3.2. Electronic properties

Using the structural study, we were able to investigate the electronic properties of t-Se with and without a defect. We calculate the electronic band structure within GGA approximation and TB-mBJ potential correction along high symmetry points in the Brillouin zone. The electronic structure of t-Se and t-Se(D) are is presented in Fig. 2a and b.

The t-Se and t-Se(D) shows an indirect band gap. The maximum of the valance band is at the L-point while the minimum of the conduction band is at the K-point as shown in Fig. 2. The DFT energy gap of t-Se is 1.087 eV using GGA and 1.516 eV using GGA-mBJ. This is significantly underestimated with respect to the experimental value of 1.85 eV [22-24]. It is remarkable that the gap of t-Se(D) is about 0.2 eV less than the t-Se gap. This behavior can be understood from the fact that when we change the rotation sense in the helical chain we put, locally, the lone pairs much closer to each other than in the normal configuration. This reduction of distance between lone pairs, in the defect neighborhood, introduces an additional Colombian repulsive energy in the system and thus reduces the energy gap [9, 11].

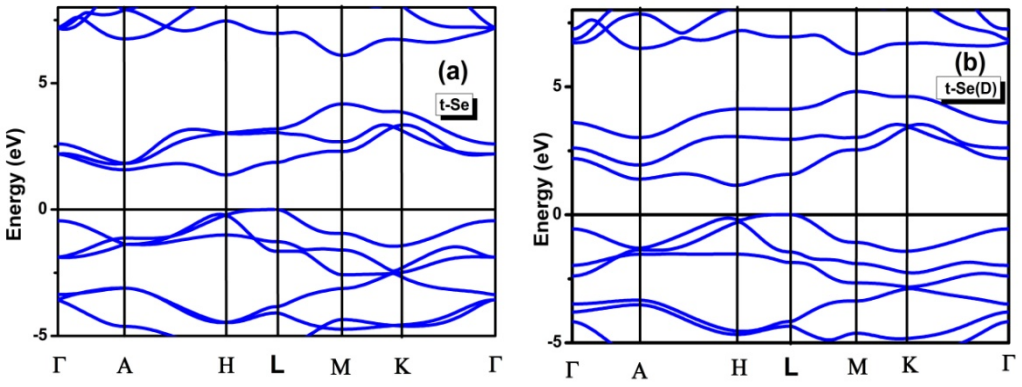

Fig. 2. Electronic band structures of : (a) t-Se, (b) t-Se(D)

The partial and total DOS of t-Se and t-Se(D) using TB-mBJ potential correction are shown in Fig. 3a, b and c. The curve a shows partial and total DOS

per atom for the atom 23 where the defect is created while curve b presents the similar partial and total DOS for the atom 11 that is far from the defect localization. The Fig. 3c. shows the total DOS for all atoms in a t-Se with and without a defect. The Fig. 4. shows the zoom of total DOS, in the region between -2.5 eV and 2.5 eV, for atoms 1, 5 and 11 of t-Se(D). The total DOS is in agreement with thus calculated in [25, 26] and the ups measurements in [27]. The total and partial DOS of all atoms show that the valence band is constructed by the p orbitals that are the p bonding states and the p lone pairs. A small hybridization with s and d states as it can be noticed, which is in agreement with other studies [26, 27]. Since the lone pairs have higher energy their states are located at the top of the valence band. The total width of the valence band is about 5.4 eV for the t-Se and 5.8 eV for the t-Se(D). The deeper states are s states and are between -9.2 eV and -15.2 eV for t-Se and -9.6 eV and -15.6 eV for t-Se(D). The conduction band is formed of the p antibonding states and a small hybridization with s and d states. This band is located between 1.52 eV and 4.17 eV for t-Se while it is located between 1.27 eV and 3.97 eV for t-Se(D).

The partial DOS of the atoms 23 and 11 in Fig. 3a and 3b show that the p orbital change of distribution especially at the valence and conduction band edges. Near the top of the valence band (-0.25 eV to 0.0 eV), the partial p DOS becomes 2 to 3 times larger and a sharp peak appears at about -0.2 eV. On the other hand, in the bottom of the conduction band edge the antibonding p states shifted to lower energies by about 0.2 eV and become much higher. Furthermore, two pronounced peaks appeared at 1.38 eV and 1.58 eV. The s and d states show a similar changes but less pronounced. These results are in agreement with another study using tight binding method [9]. The shift in p states at the conduction band edge explains the reduction of the gap by 0.2 eV as shown in the electronic structure above.

The changes in the partial p states could be attributed to the fact that at the defect location the lone pairs of two successive atoms are almost parallel rather than perpendicular like in a normal helical chain. This configuration puts negative charges closer to each other, this, of course, adds positive repulsive energy to the system. This repulsive energy weakness the covalent bonds at the defect location and this leads to push these σ bonds to higher energies near the top of the valence band making the peak at -0.2 eV. At the same time the antibonding σ^* states move to lower energies making the two sharp peaks mentioned above. The fact that the changes in the density of p states of the atom n decrease with increasing the distance between atom n and atom 23, as seen in Fig. 4., that shows partial and total DOS for different atoms, confirms that the repulsion between parallel lone pairs stand behind these changes. This phenomenon is the same regardless of whether the atom n is from the same chain as atom 23 or not as shown in Fig. 4.

for atoms 1 and 5. It is worth to indicate that the orbitals s and d behaves exactly like orbital p as shown in Fig. 3. and Fig. 4.

Using the transient photoconductivity in amorphous Selenium, the evidence of the existence of two shallow defect states levels at about 0.2 eV above the valence band edge and below the conduction band edge, as mentioned above, have been reported [11, 12]. These defect levels have been attributed to the defect in the dihedral angle which can be now confirmed by these results.

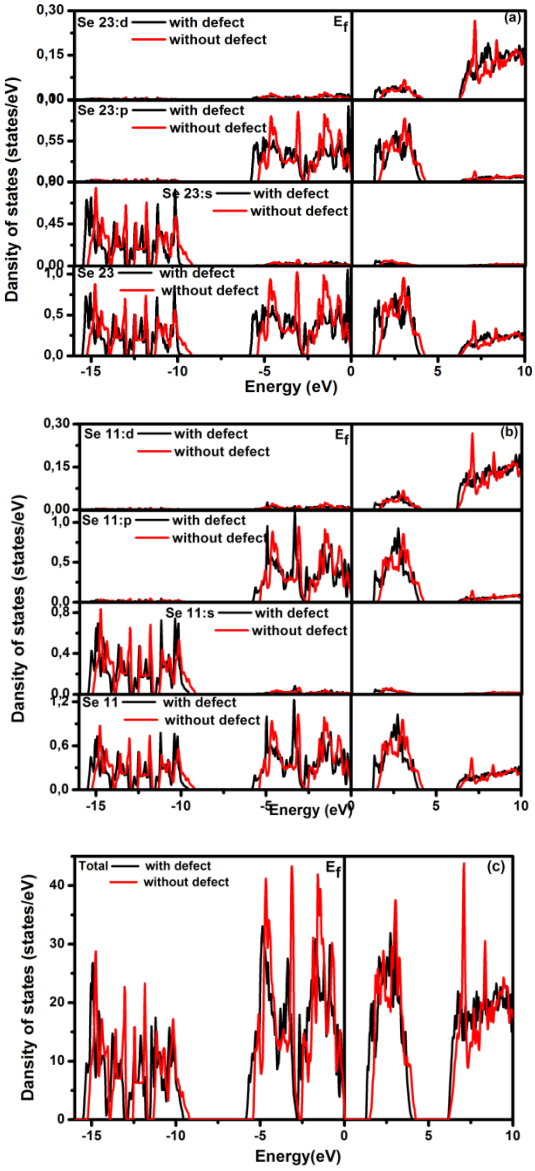

Fig. 3. The total and partial DOS for t-Se and t-Se(D) (a) for atom 23, (b) for atom 11, (c) for all atoms.

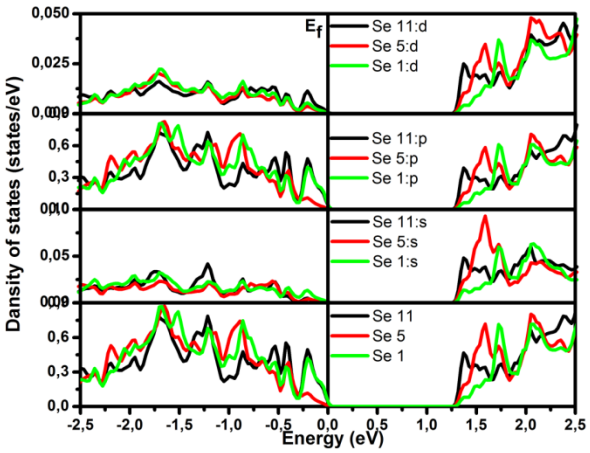

Fig. 4. The total and partial DOS for t-Se(D) for atoms 1, 5 and 11.

4. Optical properties

We can approach the optical properties using the dielectric function $\varepsilon(\omega)$ given as:

$$\varepsilon(\omega) = \varepsilon_1(\omega) + i\varepsilon_2(\omega) \tag{1}$$

Where: $\varepsilon_1(\omega)$: The real part of the dielectric function is given as [28] :

$$\varepsilon_1(\omega) = 1 + (\frac{2}{\pi})\int_0^\infty \frac{\omega'\varepsilon_2(\omega')}{(\omega'^2 - \omega^2)} d\omega' \tag{2}$$

$\varepsilon_2(\omega)$: The imaginary part of the dielectric function is given as [28] :

$$\varepsilon_2(\omega) = (\frac{4\pi e^2}{\omega^2 m^2})\sum_{i,j}\int \langle i|M|j\rangle^2 f_i(1-f_j)\delta(E_f - E_i - \omega)d^3k \tag{3}$$

The real part $\varepsilon_1(\omega)$ is presented in Fig. 5. Fig. 5a. is $\varepsilon_1(\omega)$ parallel to the c axis (zz) and Fig. 5b. is $\varepsilon_1(\omega)$ perpendicular to the c axis (xx). Fig. 5a. shows the calculated $\varepsilon_1(\omega)$ for t-Se, the calculated one for t-Se(D) and the experimental results as digitized and combined from [29, 30]. Despite the difference in the peak positions probably due to the gap underestimation, the calculated $\varepsilon_1(\omega)$ shows a good agreement with experimental results as it is seen in Table 2. The small differences are perhaps also due to imperfection in experiment procedure. Indeed the directly measured quantity is the reflection that can be disturbed by the quality of the front and back surface of the sample for example. The refractive index $n_{xx,\ zz}(0)$ that is $[\varepsilon_{1xx,\ zz}(\omega)]^{0.5}$ at 0 energy is in good agreement with experimental results [31-36].

The difference in refractive index between the two directions is $\Delta n = n_{zz}(0) - n_{xx}(0)$ is 0.645 for t-Se while it is 0.586 for t-Se(D). This indicates that the anisotropy of t-Se is larger than the anisotropy of t-Se(D). We can also see that the decrease in Δn is caused by the increase of the ε_{1xx} value due to the defect. This behavior can be explained by the difference in covalent bond component between chains as it is shown in the calculated distribution of charge density for t-Se and t-Se(D) in Fig. 6. Indeed, as seen in the Fig. 6., the effect of the defect is clear along the (0001) direction, as it can be seen from the contours of both t-Se and t-Se(D) that there are two different types of bonds, for the t-Se the charge is distributed around the atoms which indicates a weak bond of Van der waals type. On the other hand the t-Se(D) shows a distribution of charges between atoms which indicates the existence of a covalent component in the bond between chains. This explains well the decrease in Δn.

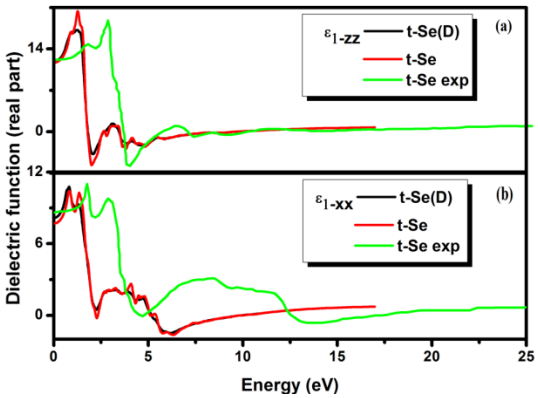

Fig. 5. The real part of the dielectric function (a) $\varepsilon_1(\omega)$ parallel and (b) $\varepsilon_1(\omega)$ perpendicular to the c axis for t-Se and t-Se(D).

Table 2

The calculated refractive index of t-Se and t-Se(D) at 0 eV and available experimental values.

	Our calculation	References					
		[31]	[32]	[33]	[34]	[35]	[36]
$n_{xx}(0)$	2.77	2.78	2.6	2.87	2.5	2.6	2.4
$n_{zz}(0)$	3.42	3.58	3.24	3.65	3.2	3.5	3.6
$n_{xx}(0)$ D	2.86	-	-	-	-	-	-
$n_{zz}(0)$ D	3.44	-	-	-	-	-	-

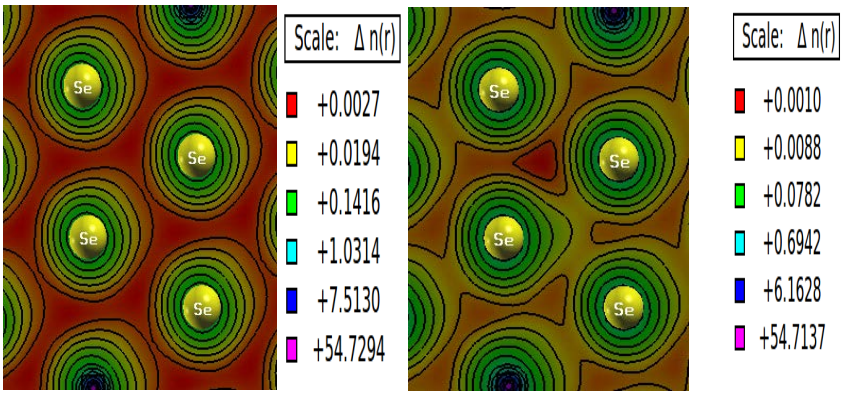

(a) (b)

Fig. 6. Valence charge density contour for (a) t-Se and (b) t-Se(D) in the (0001) plane.

Fig. 7. shows the imaginary part $\varepsilon_2(\omega)$. Fig. 7a. shows the $\varepsilon_{2zz}(\omega)$ while Fig. 7b. presents $\varepsilon_{2xx}(\omega)$. Fig. 7. Shows the calculated $\varepsilon_2(\omega)$ for t-Se, for t-Se(D) and the experimental ones. A close agreement between experimental and calculated $\varepsilon_2(\omega)$ of t-Se is observed along the all energy interval. The positions of the peaks in $\varepsilon_2(\omega)$ can be explained by the peaks in electronic structure of the valence and conduction band as seen in the DOS curves. The changes of $\varepsilon_2(\omega)$ for t-Se(D) follow the changes in the DOS structure, this appears for example in the taking off of $\varepsilon_2(\omega)$ and $\varepsilon_1(\omega)$ of t-Se(D) that is about 0.2 eV before the one of t-Se. The defect introduces more changes in perpendicular components of $\varepsilon_2(\omega)$ than the parallel components as it can be seen in Fig. 8. that show the zoom of $\varepsilon_2(\omega)$ in the region between 0 and 4 eV. The introduction of a covalent component in the bond between chains, caused by the defect, stands behind the anisotropy of changes, caused by the defect, in $\varepsilon_2(\omega)$.

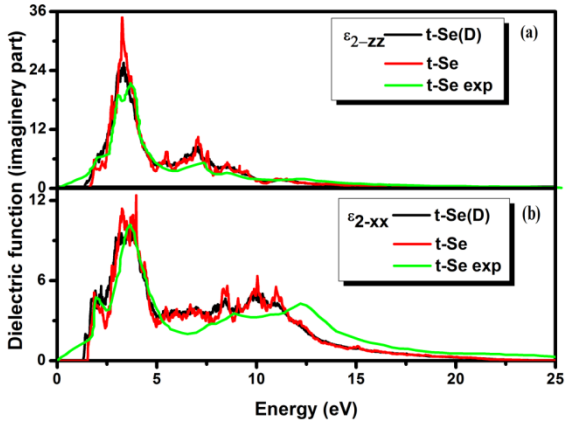

Fig. 7. The imaginary part of the dielectric function (a) $\varepsilon_2(\omega)$ parallel and (b) $\varepsilon_2(\omega)$ perpendicular to the c axis for t-Se and t-Se(D).

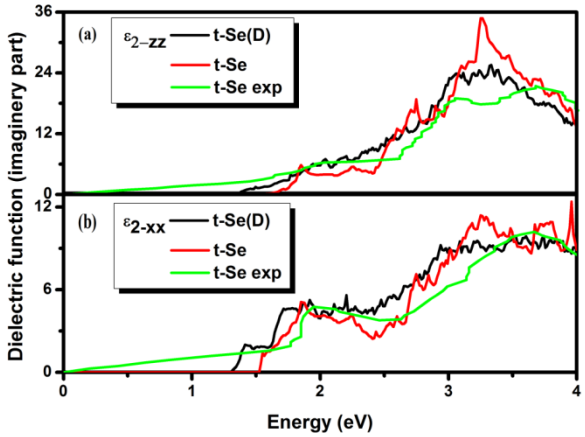

Fig. 8. The imaginary part of the dielectric function for t-Se and t-SeD from 0 to 4 eV.

5. Conclusions

We studied the effect of a defect in the dihedral angle that is a change in the rotation sense of the helical chain on the electronic and optical properties of t-Se. In this study we used the WIEN2k code based DFT using the GGA with and without the potential of correction TB-mBJ. The most important results are:

- The introduction of the defect does not change the structure parameters.
- The obtained electronic structure and DOS of t-Se are in agreement with other theoretical and experimental results.
- The gap of t-Se(D) is lower by 0.2 eV in comparison with the gap of t-Se.
- Two picks appeared in the DOS of t-Se(D) the first at -0.2 eV the second at 1.38 eV. The changes in DOS and the gap are attributed to the changes in the configuration of the lone pairs in the neighborhood of the defect. The picks could have a relation with the shallow defects in a-Se.
- Changes in refractive index and real and imaginary parts of the dielectric constants are attributed to a covalent component of inter-chain bond in the t-Se(D). The inter-chain bond in t-Se is Van der Waals type.

R E F E R EN C E S

[1] *S.O. Kasap and J.A. Rowlands.* “Review X-ray photoconductors and stabilized a-Se for direct conversion digital flat-panel X-ray image-detectors” J. Mater. Sci., Mater. Electron.11, 179 (2000). Doi:10.1023 /A:1008993813689.

[2] *J.A. Rowlands and S.O. Kasap*. "Amorphous semiconductors usher in digital x-ray imaging » Phys. Today, 24, November (1997). Doi:10.1063/ 1.881994.
[3] *S. Kasap, J.B. Frey, G. Belev*, O. Tousignant, H. Mani, J. Greenspan, L. Laperriere, O. Bubon, A. Reznik, G. DeCrescenzo, K.S. Karim, and J.A. Rowlands. "Amorphous and Polycrystalline Photoconductors for Direct Conversion Flat Panel X-Ray Image Sensors » Sensors, 11(5), 5112 (2011).
[4] *T. Nakada and A. Kunioka*. "Integrated selenium color sensor and its application to a color-recognition system » Sens. Actuators, A, 40, 117 (1994).
[5] *Shigeyuki Imura, Kenji Kikuchi, Kazunori Miyakawa, and Misao Kubota*. "Optical properties of photoconductor using crystalline selenium » Can.J.Phys.92:1–3(2014).
[6] *Madelung O., Rössler U., Schulz M.* (eds) Non-Tetrahedrally Bonded Elements and Binary Compounds I. Landolt-Börnstein - Group III Condensed Matter (Numerical Data and Functional Relationships in Science and Technology), vol 41C. Springer, Berlin, Heidelberg
[7] *V. S. Minaev, S. P. Timoshenkov, V. V. Kalugin*. « Structural and phase transformations in condensed selenium » J. Optoelectron. Adv. Mat. Vol. 7, No. 4, 2005.
[8] *S. R. Elliott*, Physics of amorphous materials (Longman, Essex,1990).
[9] *C. K. Wong G.Lucovsky J.Bernholc*. "Intrinsic localized defect states in a-Se associated with dihedral angle distortions » Journal of Non-Crystalline Solids 97–98, Part 2, 1987 .
[10] *E. V. Emelianova, M. L. Benkhedir, M. Brinza and G. J. Adriaenssens*. "Analysis of electron time-of-flight photocurrent data from a-Se."J. Appl. Physics 99 , 083702 (2006).
[11] *M L Benkhedir, M Brinza, G J Adriaenssens and C Main*. « Structure of the band tails in amorphous selenium » J. Phys.: Condens. Matter 20 (2008) 215202.
[12] *M.L. Benkhedir, M. Brinza, N. Qamhieh, G.J. Adriaenssens*. "Discrete defect levels in the amorphous selenium bandgap "Journal of Non-Crystalline Solids 352 (2006) 1543–1546.
[13] *Fadila Serdouk , Mohammed Loutfi Benkhedir*. « Density of states in pure and As doped amorphous selenium determined from transient photoconductivity using Laplace-transform method ». PhysicaB459 (2015) 122–128.
[14] Kasap S. O., Koughia C., Berashevich J., Johanson R. and Reznik A., J. Mater. Sci. Mater. Electron. 26 (2015) 4644.
[15] *Salman M. Arnab and M. Z. Kabir*, J. Appl. Phys. 122,(2017) 134502.
[16] David Koller, Fabien Tran, and Peter Blaha. "Merits and limits of the modified Becke Johnson exchange potential", Phys. Rev. B 83, 195134 2011.
[17] *P. Blaha, K. Schwarz, G. K. H. Madsen, D. Kvasnicka, and J. Luitz*, "WIEN2K: An Augmented Plane Wave plus Local Orbitals Program for Calculating Crystal Properties", Vienna University of Technology, Austria, 2001.
[18] *J.P. Perdew, K. Burke, and M. Ernzernof*, "Generalized Gradient Approximation Made Simple » Phys. Rev. Lett. 77, 3865 (1996).
[19] *F. D. Murnaghan*, "The compressibility of media under extreme pressures". Natl. Acad. Sci. USA, 30, 5390, 1944.
[20] *A. Darbandi and O. Rubel* . "Interaction of hot carriers with optical phonons in Selenium » J. Non-Cryst. Solids, 358, 2434 (2012). doi: 10.1016/j.jnoncrysol.2011.11.032
[21] *H. E. Swanson, N. T. Gilfrich, and G. M. Ugrinic*. National Bureau of Standards Circular 539, Vol.5, U. S. Government Printing Office, Washington, D. C., 1955, p 54.
[22] *R. Fischer*. Phys. "Absorption and Electroabsorption of Trigonal Selenium near the Fundamental Absorption Edge » Rev. B, 5, 3087 (1972). doi:10.1103/Phys Rev B.5.3087.
[23] *B. Moreth.* "Two Types of Indirect-Exciton Ground States in Trigonal Selenium » Phys. Rev. Lett. 42, 264 (1979). doi:10.1103/PhysRevLett.42.264.

[24] *M. Takumi, Y. Tsujioka, N. Hirai, K. Yamamoto, and K. Nagata*. "Optical absorption spectrum of trigonal selenium under high pressure'' J. Phys.: Conf. Ser. 215, 012049 (2010). doi:10.1088/1742-6596/215/1/012049.

[25] *G. Kresse, J. Furthmüller, and J. Hafner*. "Theory of the crystal structures of selenium and tellurium: The effect of generalized-gradient corrections to the local-density approximation » Phys. Rev. B 50, 13181 (1994).

[26] *J. D. Joannopoulos, M. Schluter, and Marvin L. Cohen*. "Electronic structure of trigonal and amorphous Se and Te» Phys. Rev. B, 11, 6 (1975).

[27] *I Ono, P C Grekos, T Kouchi, M Nakatake, M Tamura, S Hosokawa, H Namatame and M Taniguchi*, « A study of electronic states of trigonal and amorphous Se using ultraviolet photoemission and inverse-photoemission spectroscopies ». J. Phys.: Condens. Matter 8 (39) (1996) 7249–7261.

[28] *W. D. Lynch*, In Handbook of Opticals Constants of Solids; Palik, E. D., Ed.; Academic Press: New York. (1985) 189.

[29] *Simpex Tutihasi and Inan Chen*. « Optical Properties and Band Structure of Trigonal Selenium » Phys. Rev. 158 (3) 623-630.

[30] *P. Bammes, R. Klucker, E. E. Koch, and T. Tuomi*, "Anisotropy of the Dielectric Constants of Trigonal Selenium and Tellurium between 3 and 30 eV » phys. stat. sol. (b) 49 (1972) 561-570.

[31] *R. S. Caldwell and H. Y. Fan*, "Optical Properties of Tellurium and Selenium » Phys. Rev. 114, 664 (1959).

[32] *V. Prosser, Czech*. "The optical constants of single crystals of hexagonal selenium" J. Phys. B 10, 306 (1960).

[33] *H. Gobrecht and A. Tausend*, "Optische Eigenschaften und Bändermodell des Selens" Z. Phys. 161, 205 (1961).

[34] *F. Eckart and W. Henrion*, "Optische Untersuchungen an hexagonalen Selen-Einkristallen » Phys. Status Solidi 2, 841(1962).

[35] *M. Kastner and R. R. Forberg*, "Pressure Dependence of Reflectivity of Se: Experimental Evidence for Large Local-Field Corrections » Phys. Rev. Lett. 36, 740 (1976).

[36] *F. Nizzoli*, "Dielectric Matrix Calculations in Helical Chain Semiconductors" in The Physics of Selenium and Tellurium, edited by E. Gerlach and P. Grosse (Springer, Berlin, 1979),